slab (Fig. 4B). This complexity suggests strong stress heterogeneity in subducted slabs (*17*). However, supershear rupture during the M_w 6.7 earthquake brings its stress drop down to 32 MPa and its radiation efficiency to about 1.0 (Fig. 4B), which are much closer to values for the M_w 8.3 Okhotsk mainshock. Therefore, strong stress heterogeneity inside subducted slabs is not required to explain the 2013 Okhotsk mainshock and its M_w 6.7 aftershock. However, the difference in rupture speed (subshear versus supershear) indicates substantial spatial heterogeneity in the fracture strength or fracture energy within the slab.

Compared with shallow supershear events, this deep event has a relatively small rupture dimension and higher static stress drop (by a factor of ~10). Our estimate of high radiation efficiency ($\eta_R \approx 1.0$) during the M_w 6.7 event is also consistent with theoretical predictions of low fracture energy during supershear ruptures (*30*). This constraint of low fracture energy bears on the question of deep earthquake faulting mechanisms, which is still enigmatic (*15*, *19*). The 1994 Bolivia earthquake involved a large amount of fracture/thermal energy and radiated relatively little energy in seismic waves (*16*). In terms of energy partitioning, the supershear M_w 6.7 earthquake represents the opposite end member from the Bolivia earthquake, with almost all the available strain energy being radiated as seismic waves. This contrast is consistent with the idea of more than one rupture mechanism for deep earthquakes in slabs with different thermal states (*18*, *20*, *21*). The Okhotsk mainshock and aftershock in a cold slab ruptured with the transformational faulting mechanism, whereas the Bolivia earthquake in a warm slab was dominated by shear melting (*18*).

REFERENCES AND NOTES

1. R. Burridge, *Geophys. J. R. Astron. Soc.* **35**, 439–455 (1973).
2. D. Andrews, *J. Geophys. Res.* **81**, 5679–5687 (1976).
3. K. Xia, A. J. Rosakis, H. Kanamori, *Science* **303**, 1859–1861 (2004).
4. R. J. Archuleta, *J. Geophys. Res.* **89**, 4559–4585 (1984).
5. M. Bouchon *et al.*, *Geophys. Res. Lett.* **28**, 2723–2726 (2001).
6. M. Bouchon, M. Vallée, *Science* **301**, 824–826 (2003).
7. K. T. Walker, P. M. Shearer, *J. Geophys. Res.* **114** (B2), B02304 (2009).
8. M. Vallée, E. M. Dunham, *Geophys. Res. Lett.* **39**, L05311 (2012).
9. E. M. Dunham, R. J. Archuleta, *Bull. Seismol. Soc. Am.* **94**, S256–S268 (2004).
10. D. Wang, J. Mori, *Bull. Seismol. Soc. Am.* **102**, 301–308 (2012).
11. H. Yue *et al.*, *J. Geophys. Res.* **118**, 5903–5919 (2013).
12. M. Bouchon *et al.*, *Tectonophysics* **493**, 244–253 (2010).
13. H. Zhang, X. Chen, *Geophys. J. Int.* **167**, 917–932 (2006).
14. Y. Kaneko, N. Lapusta, *Tectonophysics* **493**, 272–284 (2010).
15. H. Houston, in *Treatise on Geophysics*, G. Schubert, Ed. (Elsevier, Amsterdam, 2007), pp. 321–350.
16. H. Kanamori, D. L. Anderson, T. H. Heaton, *Science* **279**, 839–842 (1998).
17. L. Ye, T. Lay, H. Kanamori, K. D. Koper, *Science* **341**, 1380–1384 (2013).
18. Z. Zhan, H. Kanamori, V. C. Tsai, D. V. Helmberger, S. Wei, *Earth Planet. Sci. Lett.* **385**, 89–96 (2014).
19. C. Frohlich, *Deep Earthquakes* (Cambridge Univ. Press, Cambridge, 2006).
20. D. A. Wiens, *Phys. Earth Planet. Inter.* **127**, 145–163 (2001).
21. R. Tibi, G. Bock, D. A. Wiens, *J. Geophys. Res.* **108**, 2091 (2003).
22. S.-C. Park, J. Mori, *J. Geophys. Res.* **113**, B08303 (2008).
23. M. Suzuki, Y. Yagi, *Geophys. Res. Lett.* **38**, L05308 (2011).
24. K. Kuge, *J. Geophys. Res.* **99** (B2), 2671–2685 (1994).
25. Z. Zhan, D. Helmberger, D. Li, *Phys. Earth Planet. Inter.* **232**, 30–35 (2014).
26. S. E. Persh, H. Houston, *J. Geophys. Res.* **109**, B04311 (2004).
27. A. Tocheport, L. Rivera, S. Chevrot, *J. Geophys. Res.* **112**, B07311 (2007).
28. Materials and methods are available in the supplementary materials.
29. C. J. Ammon *et al.*, *Science* **308**, 1133–1139 (2005).
30. R. Madariaga, K. B. Olsen, *Pure Appl. Geophys.* **157**, 1981–2001 (2000).
31. G. P. Hayes, D. J. Wald, R. L. Johnson, *J. Geophys. Res.* **117**, B01302 (2012).

ACKNOWLEDGMENTS

We thank two anonymous reviewers for their helpful comments. The Incorporated Research Institutions for Seismology (IRIS) provided the seismic data. This work was supported by NSF (grants EAR-1142020 and EAR-1111111). All data used are available from the IRIS data center at www.iris.edu.

SUPPLEMENTARY MATERIALS

www.sciencemag.org/content/345/6193/204/suppl/DC1
Materials and Methods
Figs. S1 to S9

27 February 2014; accepted 2 June 2014
10.1126/science.1252717

OCEAN MICROBES

Multispecies diel transcriptional oscillations in open ocean heterotrophic bacterial assemblages

Elizabeth A. Ottesen,[1,2,3] Curtis R. Young,[1,2] Scott M. Gifford,[1,2] John M. Eppley,[1,2] Roman Marin III,[4] Stephan C. Schuster,[5] Christopher A. Scholin,[4] Edward F. DeLong[1,2,6]*

Oscillating diurnal rhythms of gene transcription, metabolic activity, and behavior are found in all three domains of life. However, diel cycles in naturally occurring heterotrophic bacteria and archaea have rarely been observed. Here, we report time-resolved whole-genome transcriptome profiles of multiple, naturally occurring oceanic bacterial populations sampled in situ over 3 days. As anticipated, the cyanobacterial transcriptome exhibited pronounced diel periodicity. Unexpectedly, several different heterotrophic bacterioplankton groups also displayed diel cycling in many of their gene transcripts. Furthermore, diel oscillations in different heterotrophic bacterial groups suggested population-specific timing of peak transcript expression in a variety of metabolic gene suites. These staggered multispecies waves of diel gene transcription may influence both the tempo and the mode of matter and energy transformation in the sea.

The coordination of biological activities into daily periodic cycles is a common feature of eukaryotes and is widespread among plants, fungi, and animals, including man (*1*). Among single celled noneukaryotic microbes, diel cycles have been well documented in cyanobacterial isolates (*2*–*4*), one halophilic archaeon (*5*), and bacterial symbionts of fish and squid (*6*, *7*). Some evidence for diel cycling in microbial plankton has also been suggested on the basis of bulk community amino acid incorporation, viral production, or metabolite consumption (*8*–*10*). However, the existence of regular diel oscillations in free-living heterotrophic bacterial species has rarely been assessed.

Microbial community RNA sequencing techniques now allow simultaneous determination of whole-genome transcriptome profiles among multiple cooccurring species (*11*, *12*), enabling high-frequency, time-resolved analyses of microbial community dynamics (*12*, *13*). To better understand temporal transcriptional dynamics in oligotrophic bacterioplankton communities, we conducted a high-resolution multiday time series of bacterioplankton sampled from the North Pacific Subtropical Gyre (*14*).

To facilitate repeated sampling of the same planktonic microbial populations through time, automated Lagrangian sampling of bacterioplankton was performed every 2 hours over 3 days by using a free-drifting robotic Environmental Sample Processor (ESP) (*13*, *15*) (fig. S1). After instrument recovery, planktonic microbial RNA was extracted, purified, converted to cDNA, and sequenced to assess whole-genome transcriptome dynamics of predominant planktonic microbial populations (tables S1 and S2). The recovered cDNAs were dominated by transcripts from

[1]Department of Civil and Environmental Engineering, Massachusetts Institute of Technology, Cambridge, MA 02139, USA. [2]Center for Microbial Oceanography: Research and Education (C-MORE), University of Hawaii, Honolulu, HI 96822, USA. [3]Department of Microbiology, University of Georgia, Athens, GA 30602, USA. [4]Monterey Bay Aquarium Research Institute, Moss Landing, CA 95039, USA. [5]Singapore Centre on Environmental Life Sciences Engineering, Nanyang Technological University, 637551 Singapore. [6]Department of Biological Engineering, Massachusetts Institute of Technology, Cambridge, MA 02139, USA.
***Corresponding author. E-mail: edelong@hawaii.edu**

Prochlorococcus and several proteorhodopsin-containing or photoheterotrophic bacteria, including members of the *Pelagibacter* (SAR11), *Roseobacter*, SAR116, SAR86, and SAR324 clades (fig. S2).

Phylogenetic analysis of gene transcripts in the most abundant taxa revealed the presence of some microdiversity (figs. S3 to S8). However, the most abundant transcripts sampled at any given time point were dominated by only a few genotypes within each population that persisted throughout the sampling period. An exception was *Roseobacter*, with transcripts for two different genes (*groEL* and *dnaK*) indicating the presence of genotypes that started at a very low

Table 1. Harmonic regression results. Sequence reads are the total number assigned to each taxon bin. Transcripts are the total number of unique ortholog clusters (see table S1) with at least one mapped sequence. Periodic is the total number of sequences identified as showing 24-hour periodicity using harmonic regression. The next row shows the proportion of variance explained by 24-hour periodicity in constrained principal components analysis (PCA). The fifth row indicates the Procrustes correlation between the first two principal components from *Prochlorococcus* and other taxa (unconstrained principal components analysis as shown in Fig. 3); *P* values based on 999 permutations. Bottom row is the correlation between pairwise transcriptome similarities at each time point from *Prochlorococcus* and heterotrophic taxa based on Mantel test on Euclidean distance matrices; *P* value based on 999 permutations.

	Prochlorococcus	*Roseobacter* SAGs	SAR11	SAR116	SAR86	SAR324
Sequence reads	2,886,677	177,982	774,064	200,368	151,468	118,098
Transcripts	3045	2604	2802	2618	2367	4732
Periodic	1491	426	201	80	10	8
Constrained PCA versus 24-hour clock	0.68 (P = 0.005)	0.49 (P = 0.005)	0.24 (P = 0.005)	0.15 (P = 0.005)	0.13 (P = 0.005)	0.10 (P = 0.01)
Procrustes test versus *Prochlorococcus* PCA		0.78 (P < 0.001)	0.55 (P < 0.001)	0.70 (P < 0.001)	0.52 (P < 0.001)	0.36 (P = 0.031)
Mantel test versus *Prochlorococcus*		0.63 (P < 0.001)	0.40 (P < 0.001)	0.31 (P = 0.003)	0.26 (P = 0.005)	0.27 (P = 0.002)

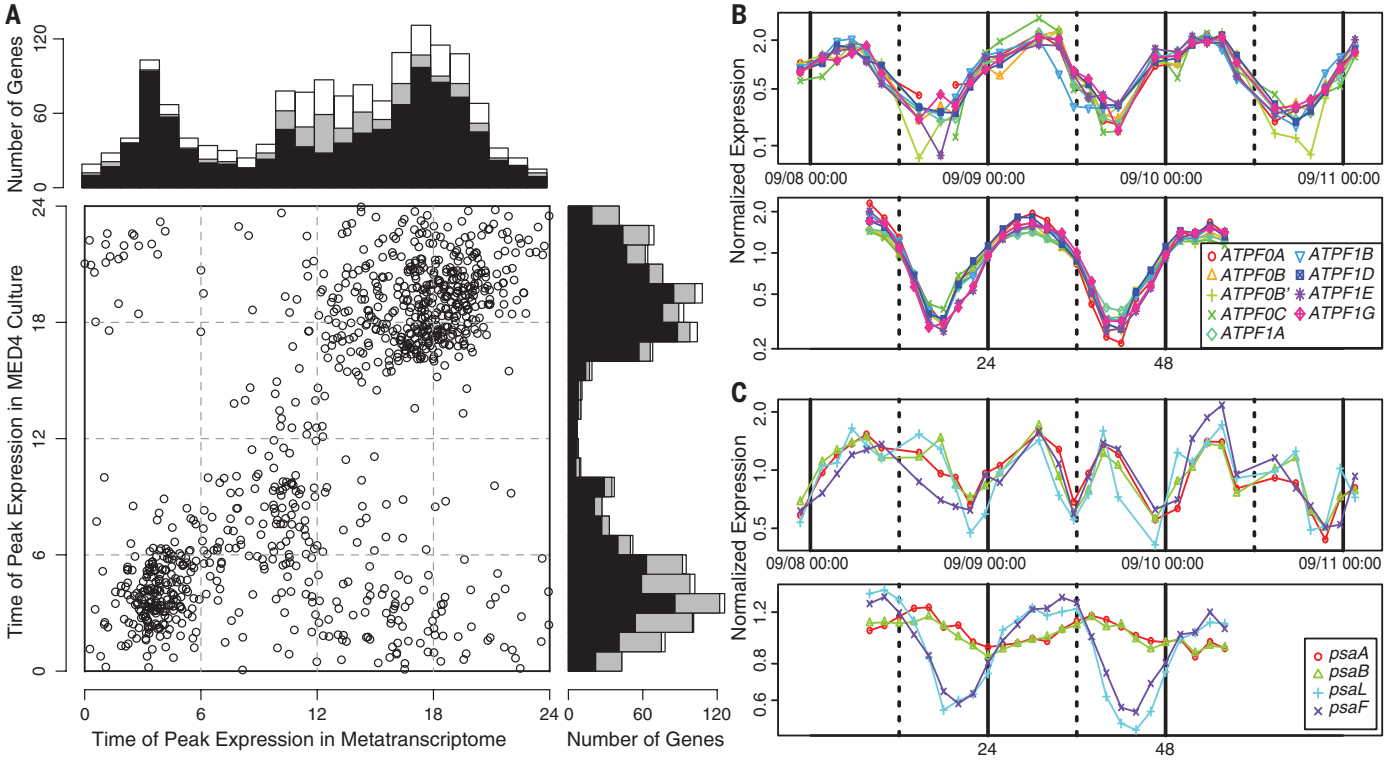

Fig. 1. Laboratory versus field comparisons of periodic expression patterns in *Prochlorococcus* populations. (**A**) Scatter plot shows time of peak abundance for 973 transcripts identified as significantly periodic in both studies. Histograms show the total number of genes peaking in 1-hour intervals in this study (top) and the laboratory experiment (side). Black bars represent genes identified as significantly periodic in both studies, gray bars represent genes expressed in both studies but significantly periodic in only one, and white bars represent significantly periodic transcripts that were not detected in the other data set. For this comparison, we used published significance cutoffs from the laboratory study (*4*) but for consistency generated new peak times by using our harmonic regression approach and the published normalized mean expression levels for each time point. In general, the peak times generated using our approach closely matched published values for that data set. (**B** and **C**) Plots showing relative expression (normalized to mean expression level) over time for our metatranscriptome (top trace) and in microarray data (bottom trace) for selected transcripts. For comparison, experimental midnights (24 and 48 hours) from the microarray study are aligned with the 12:00 midnight samples from 9 and 10 September, respectively. All adenosine triphosphate (ATP) synthase subunits (B) and selected subunits from photosystem I (C) are shown.

abundance and increased in representation over the course of the time series. This variability could be due to an injection of a new population as water masses mixed during the latter portion of the time series or to an alteration in the relative transcriptional activities of two ecotypes that are responding to changes in the surrounding environment.

Transcriptional activity in *Prochlorococcus* was highly dependent on the time of day. Harmonic regression analyses indicated that nearly half (1491) of all *Procholorococcus* population transcripts were significantly periodic (Table 1, table S3, and Fig. 1). The expression patterns observed were similar to those of monocultures growing in controlled laboratory settings (*4*), but there were also notable differences (Fig. 1). For example, photosystem I gene expression exhibited a double peak in the wild *Prochlorococcus* transcriptome around noon (Fig. 1). In contrast, under laboratory conditions most photosystem I genes, for example, *psaL* and *psaF*, were found to peak just before noon, and *psaA* and *psaB* peaked shortly after noon (*4*).

The largest discrepancy between *Prochlorococcus* laboratory studies and our field observations was that a considerable number of *Prochlorococcus* transcripts in our field populations peaked around midday (Fig. 1). Some of these genes did exhibit periodicity in cultures but peaked at a different time of day than in field populations. A larger fraction of the field midday-peaking transcripts were either not periodically expressed or were not present in the culture experiments. In addition, 62% of the 10 a.m.–to–4 p.m. peaking transcripts in our field study lacked Kyoto Encyclopedia of Genes and Genomes (KEGG) orthology annotations, as opposed to those peaking in the evening or late at night.

A number of factors may be responsible for differences in transcript dynamics between in laboratory cultures versus field *Prochlorococcus* populations. Maximal light levels at our study site at 23-m depth were frequently twofold higher (450 μmol Q m^{-2} s^{-1}) than those used in laboratory microarray experiments (232 μmol Q m^{-2} s^{-1}) (*4*). Fundamental genetic differences between our field populations and the *Prochlorococcus* strain used in laboratory culture experiments likely also contribute to the differences we observed. Other variables, including nutrient composition and organismal interactions, may also be factors in the observed differences. Although we could not identify obvious trends in the type or function of field population transcripts showing peak expression during the midday period, they did include a wide range of enzymatic functions that are more consistent with nutrient-responsive metabolic changes rather than a simple high-light stress response.

An abundant *Roseobacter* population also showed strong diel oscillations in its transcriptome profile, most notably in expressed genes involved in bacteriochlorophyll-associated aerobic anoxygenic photosynthesis. Overall, a large fraction of *Roseobacter* transcripts were periodically expressed (Table 1). Of these, the majority peaked during daylight hours, with only a few gene transcripts peaking at night (Fig. 2). Although this pattern contrasts with that observed in *Prochlorococcus*, where most diurnally regulated transcripts peaked at dawn or dusk, it was consistent with transcriptional regulation recently reported in *Dinoroseobacter shibae* (*16*).

Thirty-five of the 40 significantly periodic *Roseobacter* transcripts that peaked between 11 p.m. and 7 a.m. encoded genes belonging to a large photosynthetic "superoperon" (fig. S9). Nightly expression of these genes, followed by immediate repression upon light onset, is consistent with the *D. shibae* study (*16*) and may be preparing cells for efficient solar energy harvest in the early morning hours. Functions that peaked during the daytime hours included ribosomal proteins, respiratory transcripts, genes involved in amino acid metabolism, and transporters (Fig. 2).

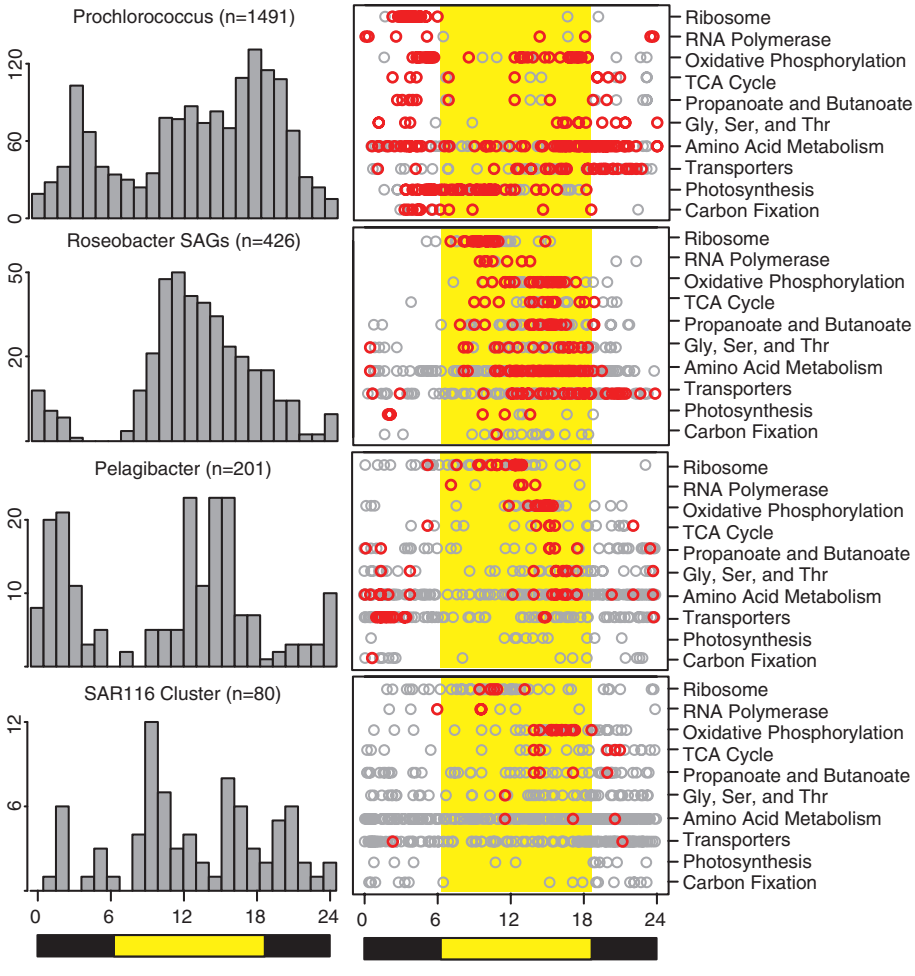

Fig. 2. Timing of periodically expressed transcripts. For each population, a histogram showing the number of periodically expressed diel transcripts with peak expression within 1-hour intervals throughout the day is shown (**left**). (**Right**) Time of peak expression of all transcripts assigned to selected KEGG pathways is plotted (gray circles). Red circles denote transcripts identified as significantly periodic (24-hour period). The transporters category includes both the ATP binding cassette transporters KEGG pathway and the transporters BRITE hierarchy; the photosynthesis category includes both the photosynthesis KEGG pathway and the BRITE photosynthesis proteins categorizations. Carbon fixation refers to genes assigned to the carbon fixation in photosynthetic organisms KEGG pathway. The photosynthesis and carbon fixation categories are present in heterotrophic organisms because of cross-assignment of ATP synthase genes and pentose phosphate cycle genes. Black and yellow bars depict the daily photoperiod (based on sunrise and sunset times). SAGs, single amplified genome-similar transcripts; TCA, tricarboxylic acid.

Proteorhodopsin-containing photoheterotrophs including Pelagibacter (SAR11), SAR116, and SAR86 also showed evidence of diel periodicity in many of their gene transcripts (Fig. 2 and Table 1). All opsin-containing bacteria analyzed (SAR11, SAR116, SAR86, and SAR324) exhibited statistically significant diel oscillations in their proteorhodopsin gene transcripts (table S3 and fig. S10). Peak expression of the opsin transcripts occurred near dawn in all these populations (fig. S10), potentially optimizing solar energy capture by the light-driven, proton-pumping rhodopsins.

Principal components analysis distinguished time series samples for each heterotroph by time of day (Fig. 3) and showed significant correlation with the light-driven behavior of *Prochlorococcus* (Table 1). Overall, these data are consistent with genome-wide transcriptional changes across the day-night cycle for each population. In addition, coclustering of transcripts using GeneARMA (GA) (*14*, *17*) revealed suites of gene transcripts that exhibited similar expression patterns among different taxa (Fig. 4, figs. S11 to S14, and table S4). For example, a group of transcripts that fit highly similar GA expression models across multiple species included Pro GA5, Pro GA7, Pro GA9, Pro GA23, SAR11 GA6, SAR11 GA18, SAR116 GA2, and *Roseobacter* GA8 (Fig. 4, fig. S14, and table S4). These multispecies, day-peaking transcripts (fig. S14 and table S4) included gene products associated with respiration (*Procholorococcus*, SAR11, SAR116, and *Roseobacter*), nitrogen metabolism (*Procholorococcus*, SAR11, and SAR116), glycine metabolism (*Procholorococcus*, SAR11, and *Roseobacter*), carbon monoxide metabolism (SAR116 and *Roseobacter*), and DNA synthesis (*Procholorococcus* and *Roseobacter*). The coclustering of gene transcripts revealed a complex pattern of expression through the day and across the time series and provides evidence for parallel trends in gene expression across multiple species (Fig. 4, fig. S11 to S14, and table S4).

Together, the transcriptional profiles of *Roseobacter*, SAR11, SAR116, and SAR86 indicate diel cycling of metabolic gene transcripts and suggest a multispecies wavelike progression of up-regulated gene suites across the day-night cycle (Fig. 4). Most conspicuously, a regular diel succession of translational, transcriptional, and respiratory gene transcripts was followed by peaks in transporter transcripts that possibly reflect a metabolic recovery phase (Fig. 2). Many of these metabolic pathway transcripts peaked earlier in the day in *Roseobacter* field populations relative to other bacterial heterotrophs (Figs. 2 and 4 and table S4).

The overall transcriptional profile of SAR324 did not show as many transcript diel oscillations as other heterotrophic taxa. Instead, principal components analysis clustered SAR324 transcripts according to the specific day that they were collected (Fig. 3). In particular, the SAR324 group showed a strong separation between the first portion of the time series and the second in principal components analysis (Fig. 3). This split appears to be associated with the increases in temperature and salinity observed across the time series (fig. S1).

The diurnal patterns reported here for open-ocean heterotrophic bacterioplankton were different from those observed in a previous study of phylogenetically related coastal bacterioplankton using similar methods (*12*). For example, coastal versus open-ocean SAR11 populations revealed differential expression levels among several orthologous transcript categories (fig. S15). Additionally, whereas the open-ocean SAR11 populations reported here exhibited statistically significant diel oscillations for many gene transcripts (Fig. 2), the coastal SAR11 populations did not.

Currently available data are insufficient to provide definitive mechanistic explanations for the diel behaviors we observed in different heterotrophic bacterioplankton species. It is possible that photoreceptors in these bacteria are involved in regulating light-dark cycles of transcriptional activity. Marine *Roseobacter* species have previously been shown to regulate their global transcriptional behavior in response to light (*16*), and laboratory cultures of *Pelagibacter* also exhibit light-responsive metabolic behaviors (*18*). However, differences between the behaviors of SAR11 coastal versus open ocean field populations (fig. S15), as well as comparisons of several taxa in our field study versus laboratory experiments on related cultivated isolates (Fig. 1), suggest that other factors may be at play in regulating diel behavior among these different bacterioplankton populations.

Previous studies have proposed that tight metabolic coupling between primary producers and consumers in microbial plankton might elicit conspicuous diel cycling in heterotrophic bacterial activities (*8*). The diel cycling we observed among different bacterioplankton species is consistent with this hypothesis, with multiple coexisting heterotroph populations exhibiting diurnal oscillations resembling those of their photoautotrophic neighbors. We postulate that the tightly coupled multispecies temporal expression patterns observed may elicit corresponding waves of species-specific metabolic responses at regular time intervals, potentially coordinating diverse biogeochemical activities in these complex microbial communities. Such temporal coordination of biogeochemical activities among multiple species may be important regulators of both the tempo and the mode of microbial matter and energy transformation in the sea.

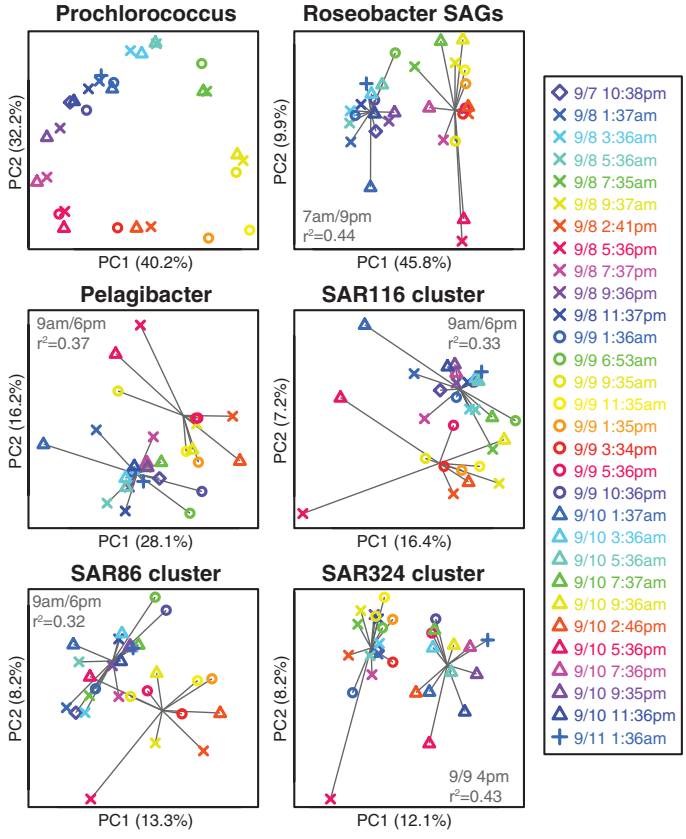

Fig. 3. Principal component (PC) analyses of population transcriptional profiles. Transcript abundances were normalized to total transcripts assigned to each population at each time point and arcsin-transformed to approximate normality (*19*). Symbol color denotes time of day, and shape denotes day of collection. Gray lines connect samples to centroids for selected sample groupings that separate points well. *Roseobacter* SAG represents samples that were collected between 7 a.m. and 9 p.m. (versus 9 p.m to 7 a.m.); Pelagibacter, SAR116, and SAR86 clusters represent samples that were collected between 9 a.m. and 6 p.m. (and vice versa); SAR324 cluster represents samples that were collected before or after 9 September 4 p.m. All factor correlations shown were highly significant (P = 0.001). Alternative time of day categories were also highly significant for *Roseobacter* SAGs, Pelagibacter, SAR116, and SAR86. SAR116 (r^2 = 0.10, P = 0.037) and SAR86 (r^2 = 0.12, P = 0.019) also correlated weakly with the grouping shown for SAR324. All analyses carried out by using functions in the vegan software package (*20*).

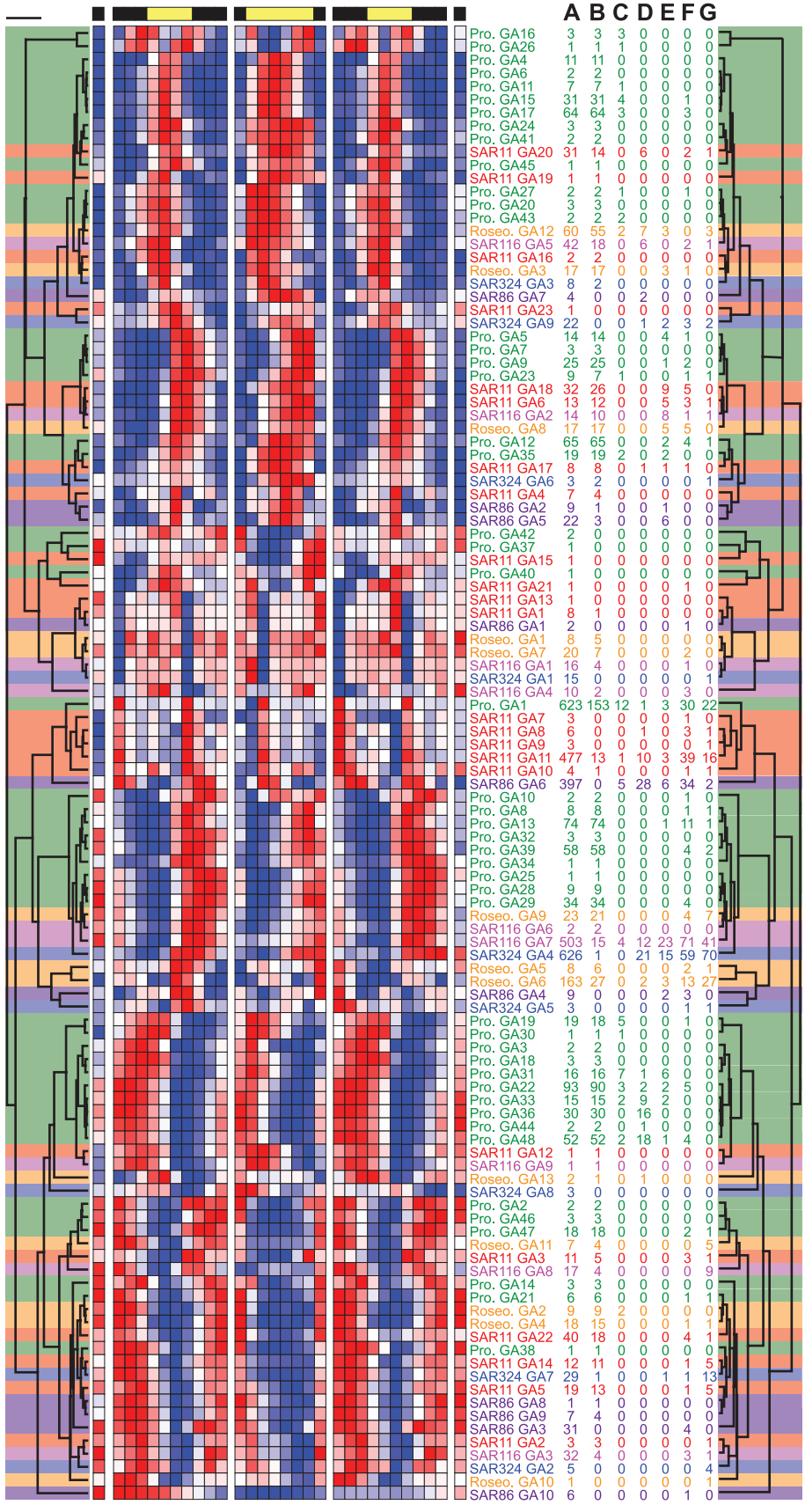

Fig. 4. Timing of expression of functional gene clusters among different taxa, clustered by the similarities of their temporal expression patterns. Heat map shows cluster models for all GA clusters, colored by mean-centered relative expression (red, high; blue, low). Black and yellow bars show the daily photoperiod. Each box represents a single sampling event; for sample times, see table S1. Dendrograms show cluster model similarity (Pearson correlations, average linkage clustering, scale bar at upper right represents a correlation of 0.5). The total number of genes (column A), significantly periodic genes (B), and genes associated with photosynthesis (C), ribosome (D), oxidative phosphorylation (E), amino acid metabolism (F), and transport (G) (defined as for Fig. 2), are listed for each cluster. See table S4 for the identities of genes found within any specific GeneARMA (GA) cluster.

REFERENCES AND NOTES

1. D. Bell-Pedersen *et al.*, *Nat. Rev. Genet.* **6**, 544–556 (2005).
2. I. M. Axmann, S. Hertel, A. Wiegard, A. K. Dörrich, A. Wilde, *Mar. Genomics*, (2014).
3. H. Ito *et al.*, *Proc. Natl. Acad. Sci. U.S.A.* **106**, 14168–14173 (2009).
4. E. R. Zinser *et al.*, *PLOS ONE* **4**, e5135 (2009).
5. K. Whitehead, M. Pan, K. Masumura, R. Bonneau, N. S. Baliga, *PLOS ONE* **4**, e5485 (2009).
6. J. F. Flint, D. Drzymalski, W. L. Montgomery, G. Southam, E. R. Angert, *J. Bacteriol.* **187**, 7460–7470 (2005).
7. A. M. Wier *et al.*, *Proc. Natl. Acad. Sci. U.S.A.* **107**, 2259–2264 (2010).
8. J. M. Gasol *et al.*, *Mar. Ecol. Prog. Ser.* **164**, 107–124 (1998).
9. C. Winter, G. J. Herndl, M. G. Weinbauer, *Aquat. Microb. Ecol.* **35**, 207–216 (2004).
10. M. Galí *et al.*, *Global Biogeochem. Cycles* **27**, 620–636 (2013).
11. S. M. Gifford, S. Sharma, M. Booth, M. A. Moran, *ISME J.* **7**, 281–298 (2013).
12. E. A. Ottesen *et al.*, *Proc. Natl. Acad. Sci. U.S.A.* **110**, E488–E497 (2013).
13. E. A. Ottesen *et al.*, *ISME J.* **5**, 1881–1895 (2011).
14. Materials and methods are available as supplementary materials on *Science* Online.
15. C. M. Preston *et al.*, *PLOS ONE* **6**, e22522 (2011).
16. J. Tomasch, R. Gohl, B. Bunk, M. S. Diez, I. Wagner-Döbler, *ISME J.* **5**, 1957–1968 (2011).
17. N. Li *et al.*, *PLOS ONE* **5**, e9894 (2010).
18. L. Steindler, M. S. Schwalbach, D. P. Smith, F. Chan, S. J. Giovannoni, *PLOS ONE* **6**, e19725 (2011).
19. Z. Liu, W. Hsiao, B. L. Cantarel, E. F. Drábek, C. Fraser-Liggett, *Bioinformatics* **27**, 3242–3249 (2011).
20. J. Okansen *et al.*, Package "vegan": Community ecology package (2012); http://cran.rproject.org/web/packages/vegan//vegan.pdf.

ACKNOWLEDGMENTS

We thank the officers and crew of the *Kilo Moana*, J. Robidart, S. Wilson, and the ESP engineering and science team (J. Ryan, J. Birch, C. Preston, G. Massion, S. Jensen, and B. Roman) for all of the able assistance. This work was supported by grants from the Gordon and Betty Moore Foundation GBMF nos. 492.01 and 3777 (E.F.D.) and NSF grant EF0424599 (E.F.D.). Development of the ESP was supported by NSF grant OCE-0314222 (to C.A.S.), NASA Astrobiology grants NNG06GB34G and NNX09AB78G (to C.A.S.), the Gordon and Betty Moore Foundation nos. 731 and 2728 (C.A.S.), and the David and Lucile Packard Foundation. This work is a contribution of C-MORE. Sequences reported in this paper have been deposited in the GenBank database (accession no. SRP041215). The Monterey Bay Aquarium Research Institute holds rights to C. A. Scholin *et al.*, U.S. Patent 6187530 (2001). C.A.S. is disqualified from receiving any royalties that might arise from licensing agreements. The ESP is available commercially from Spyglass Technologies and MacLane Research Laboratories; C.A.S. has no financial interest in either company and is not compensated in any way for giving advice on ESP technology transfer.

SUPPLEMENTARY MATERIALS

www.sciencemag.org/content/345/6193/207/suppl/DC1
Materials and Methods
Figs. S1 to S14
Tables S1 to S4
References (*21*–*35*)

20 February 2014; accepted 22 May 2014
10.1126/science.1252476

MICROECONOMICS

Harnessing naturally occurring data to measure the response of spending to income

Michael Gelman,[1] Shachar Kariv,[2] Matthew D. Shapiro,[1,3]* Dan Silverman,[3,4] Steven Tadelis[3,5]

This paper presents a new data infrastructure for measuring economic activity. The infrastructure records transactions and account balances, yielding measurements with scope and accuracy that have little precedent in economics. The data are drawn from a diverse population that overrepresents males and younger adults but contains large numbers of underrepresented groups. The data infrastructure permits evaluation of a benchmark theory in economics that predicts that individuals should use a combination of cash management, saving, and borrowing to make the timing of income irrelevant for the timing of spending. As in previous studies and in contrast to the predictions of the theory, there is a response of spending to the arrival of anticipated income. The data also show, however, that this apparent excess sensitivity of spending results largely from the coincident timing of regular income and regular spending. The remaining excess sensitivity is concentrated among individuals with less liquidity.

Economic researchers and policy-makers have long sought high-quality measures of individual income, spending, and assets from large and heterogeneous samples. For example, when policy-makers consider whether and how to stimulate the economy, they need to know how individuals will react to changes in their income. Will individuals spend differently? Will they save at a different rate or reduce their debt, and when? There are many obstacles to obtaining reliable answers to these important questions. One obstacle is that existing data sources on individual income and spending have substantial limits in terms of accuracy, scope, and frequency.

This paper advances the measurement of income and spending with new high-frequency data derived from the actual transactions and account balances of individuals. It uses these measures to evaluate the predictions of a benchmark economic theory that states that the timing of anticipated income should not matter for spending. Like previous research, it finds that there is a response of spending to the arrival of anticipated income. The data show that, on average, an individual's total spending rises substantially above average daily spending on the day that a paycheck or Social Security check arrives, and remains high for at least the next 4 days. The data also allow the construction of variables that show, however, that this apparent excess sensitivity of spending results in large part from the coincident timing of regular income and regular spending. The remaining excess sensitivity is concentrated among individuals who are likely to be liquidity-constrained.

Traditionally, researchers have used surveys such as the Consumer Expenditure Survey (CEX) to measure individual economic activity. Such surveys are expensive to implement and require considerable effort from participants and are therefore fielded infrequently, with modest-sized samples. Researchers have recently turned to administrative records, which are accurate and can be frequently refreshed, to augment survey research. So far, however, the administrative records have typically represented just a slice

Table 1. Check versus ACS demographics (percent). The sample size for Check is 59,072, 35,417, 28,057, and 63,745 for gender, age, education, and region, respectively. The sample size for ACS is 2,441,532 for gender, age, and region and 2,158,014 for education.

	Check	ACS
Sex		
Male	59.93	48.59
Female	40.07	51.41
Age		
18–20	0.59	5.72
21–24	5.26	7.36
25–34	37.85	17.48
35–44	30.06	17.03
45–54	15.00	18.39
55–64	7.76	16.06
65+	3.48	17.95
Highest degree		
Less than college	69.95	62.86
College	24.07	26.22
Graduate school	5.98	10.92
Census Bureau region		
Northeast	20.61	17.77
Midwest	14.62	21.45
South	36.66	37.36
West	28.11	23.43

[1]Department of Economics, University of Michigan, Ann Arbor, MI 48109, USA. [2]Department of Economics, University of California, Berkeley, Berkeley, CA 94720, USA. [3]National Bureau of Economic Research (NBER), Cambridge, MA 02138, USA. [4]Department of Economics, Arizona State University, Tempe, AZ 85287, USA. [5]Haas School of Business, University of California, Berkeley, Berkeley, CA 94720, USA.
*Corresponding author. E-mail: shapiro@umich.edu

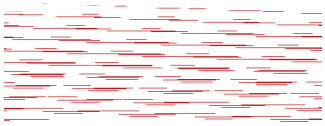

Multispecies diel transcriptional oscillations in open ocean heterotrophic bacterial assemblages

Elizabeth A. Ottesen, Curtis R. Young, Scott M. Gifford, John M. Eppley, Roman Marin III, Stephan C. Schuster, Christopher A. Scholin and Edward F. DeLong (July 10, 2014)

Science **345** (6193), 207-212. [doi: 10.1126/science.1252476]

Editor's Summary

Up and down go the cyanobacteria

Plankton move together in strikingly coordinated daily patterns, sinking at night to avoid being eaten and rising to the surface in daylight to photosynthesize. Otteson *et al.* found similar activity patterns in even the smallest of planktonic organisms, such as photosynthetic bacteria (see the Perspective by Armbrust). Because it's hard to take regular samples in the open ocean, the authors built a robotic sampler and set it adrift for several days in the mid-Pacific. The captured bacteria showed immediate responses to changes in light, temperature, and salinity in ways that could affect the ocean's carbon and nitrogen cycles.

Science, this issue p. 207; see also p. 134

Science (print ISSN 0036-8075; online ISSN 1095-9203) is published weekly, except the last week in December, by the American Association for the Advancement of Science, 1200 New York Avenue NW, Washington, DC 20005.